



DOI:10.22144/ctujoisd.2025.004

## Recycling used coffee grounds as fine aggregate in alkali-activated lightweight non-load-bearing composites

Huynh Quoc Dung, Luong Hoang Nhat Huy, Ngo Nhat Tan, Duong Thanh Hau, Nguyen Thanh Binh, Lam Tri Khang, and Trong-Phuoc Huynh\*

Faculty of Civil Engineering, College of Engineering, Can Tho University, Viet Nam

\*Corresponding author (htphuoc@ctu.edu.vn)

### Article info.

Received 31 Jul 2024  
Revised 23 Aug 2024  
Accepted 12 Feb 2025

### Keywords

ANLC, compressive strength, dry density, used coffee ground, water absorption

### ABSTRACT

Coffee is one of the most consumed drinks, which releases large amounts of used coffee grounds (UCG), causing environmental problems. Thus, UCG was re-used in combination with bottom ash (BA) as fine aggregates in making alkali-activated non-load-bearing lightweight composites (ANLC) in this study. To evaluate the effect of UCG on the properties of ANLC, seven ANLC mixtures with UCG/BA ratios of 0/100, 5/95, 10/90, 15/85, 20/80, 25/75, and 30/70 were prepared. Results showed that the properties of ANLC were influenced significantly by UCG contents. Indeed, an increase in UCG content led to a decrease in dry density, strength, and drying shrinkage while increasing the ANLC's water absorption, except for the specimen with 5% UCG incorporation. Correlations among properties of ANLC were established and the potential applications of ANLC in real practice were also suggested, proving that the ANLC could be applied to non-load-bearing elements. Among the mixtures, the 28-day ANLC specimen containing 5% UCG exhibited the highest flexural and compressive strengths of 7.12 MPa and 39.4 MPa, respectively, and the lowest water absorption of 10.29% with the relatively low dry density of 1671 kg/m<sup>3</sup>, indicating the feasibility of using UCG as fine aggregate in the production and application of ANLC.

## 1. INTRODUCTION

Coffee consumption has risen in recent decades, driven by a growing demand across various cultures and economic sectors. According to Torga and Spers (Torga & Spers, 2020), global coffee consumption reached approximately 7.5 million tonnes in 2016. In 2018, coffee production was over 9.5 billion kg and the coffee demand was expected to triple in 2050 (Nab & Maslin, 2020). Particularly, Vietnam has the second-highest annual coffee production in the world, only behind Brazil (Ghosh & Venkatachalapathy, 2014). Due to high demand, coffee is one of the most consumed beverages, resulting in the generation of large quantities of used

coffee grounds (UCG). Each kilogram of coffee beans used produces 1.88 kg of UCG. The primary sources of UCG are the soluble coffee industry and consumption in catering outlets and homes (Rivera et al., 2020). Thus, UCG is often sent to landfills, resulting in food loss and waste problems, which not only contribute to carbon emissions but also represent a loss of potentially valuable organic material (Saberian et al., 2021). Therefore, it is essential to develop strategies to minimize UCG for both economic and environmental reasons toward sustainable development goals. In recent years, UCG has been investigated for its usage in construction applications as a natural sand replacement in mortar production (Scalia et al.,

2021), as raw material in ceramic clay brick (Moussa et al., 2022), floor tile (Busch & França Holanda, 2022), and concrete production (Roychand et al., 2023).

Although prior studies have shown the potential use of UCG in construction applications, it is frequently used as a substitute for fine aggregate owing to its small particle size and low density. Furthermore, these characteristics make UCG well-suited for use in producing alkali-activated non-load-bearing lightweight composite (ANLC), which is formed through chemical reactions between aluminosilicate sources and alkaline activators, rather than using traditional Portland cement (John et al., 2021). With the rapid development of industrialization, an increasing number of projects are using ANLC to reduce weight and optimize construction costs for structural components. High-rise buildings are a notable example of this trend. In addition to reducing the weight of the structures, the use of ANLC also helps to cut down a significant amount of CO<sub>2</sub> by limiting the use of cement. In recent years, alkali-activated lightweight composites have been researched to enhance their technical properties and optimize production costs. For example, Darvish et al. (2020) reported that using palm oil clinker as a sand replacement in geopolymer mortar could reduce the drying shrinkage. Gencel et al. (2021) investigated the use of vermiculite as a sand replacement in geopolymer mortar. Their findings indicated that incorporating expanded vermiculite into the geopolymer mortar results in eco-friendly and lightweight building composites with enhanced sound and thermal insulation properties. Suksiripattanapong et al. (2020) used BA from Mae Moh electrical power plant in lightweight geopolymer mortar. They found that the density of lightweight geopolymer mortar was decreased with the replacement of BA.

Although sand in geopolymer mortar is replaced by various materials, the use of UCG in the ANLC field is still a relatively new concept. Therefore, to fulfill this gap in the literature sources, the present study explored the feasibility of utilizing UCG in ANLC, offering a sustainable alternative to traditional construction materials. By examining the properties (i.e., density, flexural strength, compressive strength, drying shrinkage, and water absorption) and potential applications of ANLC incorporating UCG, the study aims to contribute to the development of eco-friendly building practices and sufficient waste management solutions for sustainable development in the construction industry.

## 2. MATERIALS AND METHODS

### 2.1. Materials and mixture proportions

#### 2.1.1. Binders

Fly ash (FA) and ground granulated blast-furnace slag (GGBFS) were used as the binder materials with the major chemical compositions, as shown in Table 1, and specific gravities of 2.27 and 2.85 g/cm<sup>3</sup>, respectively. Previous research indicates that the available SiO<sub>2</sub>, Al<sub>2</sub>O<sub>3</sub>, and CaO in FA and GGBFS positively influence the polymerization process, enhancing the performance of alkali-activated materials through the formation of calcium-aluminate-silicate-hydrate (C-A-S-H) and sodium-calcium-alumino-silicate-hydrate (N(C)-A-S-H) phases (Zeyad et al., 2020; Srividya et al., 2022). Besides, the alkaline activator prepared for ANLC was a combination of sodium hydroxide 5M (SH) and sodium silicate (SS) solutions. SH and SS had respective densities of 1.19 and 1.38 g/cm<sup>3</sup>.

**Table 1. Chemical compositions of FA and GGBFS**

Composition (wt.%)	FA	GGBFS
SiO <sub>2</sub>	50.3	33.9
Al <sub>2</sub> O <sub>3</sub>	35.6	14.4
Fe <sub>2</sub> O <sub>3</sub>	5.2	-
CaO	1.2	40.8
MgO	0.8	6.7
SO <sub>3</sub>	0.2	1.2
K <sub>2</sub> O	1.9	0.5
Na <sub>2</sub> O	0.3	0.4
Others	4.5	2.1

#### 2.1.2. Aggregates



**Figure 1. The natural appearance of UCG**

In this study, the aggregate used for making ANLC specimens was a combination of coal bottom ash (BA, fineness modulus (FM) of 2.42, water absorption of 8.2%, and density of 2.15 g/cm<sup>3</sup>) and UCG

(Figure 1, FM of 2.24, water absorption of 88.7%, and density of 1.25 g/cm<sup>3</sup>). It is important to note that both BA and UCG were used in saturated surface dry form, and the grain size distributions of these materials are displayed in Figure 2.

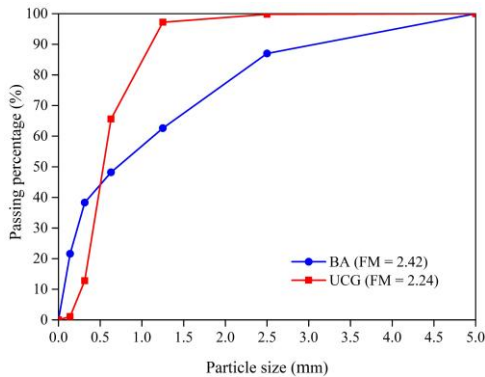


Figure 2. Grain size distributions of aggregates

Table 2. Material proportions for 1 m<sup>3</sup> ANLC

Mixtures	C00	C05	C10	C15	C20	C25	C30
FA (kg)	186.8	186.8	186.8	186.8	186.8	186.8	186.8
GGBFS (kg)	436.0	436.0	436.0	436.0	436.0	436.0	436.0
NaOH (kg)	150.6	150.6	150.6	150.6	150.6	150.6	150.6
Na <sub>2</sub> SiO <sub>3</sub> (kg)	93.9	93.9	93.9	93.9	93.9	93.9	93.9
Water (kg)	135.6	135.6	135.6	135.6	135.6	135.6	135.6
BA (kg)	934.2	887.5	840.8	794.1	747.4	700.7	654.0
UCG (kg)	0.0	27.2	54.3	81.5	108.6	135.8	163.0

2.2. Sample preparation and test methods

2.2.1. Sample preparation

The sample preparation processes comprised four main stages: Initially, all materials were prepared based on the proportions detailed in Table 2. The activator solution was created by mixing SH and SS. In the second stage, FA and GGBFS were dry-mixed for 2 min using a laboratory mixer, after which the activator solution was slowly poured into the mixer and the mixture was then continuously mixed for another 3 minutes to achieve a homogeneous binder. Subsequently, BA and UCG were added to the mixer, followed by mixing water to adjust the workability of the fresh mixture. In the final stage, the fresh mixture was poured into molds with different dimensions to prepare ANLC specimens. After 24 hours, the specimens were demolded and allowed to cure in the air until the testing days.

2.2.2. Test methods

After being cured, ANLC specimens were tested for density, flexural and compressive strength, drying

2.1.3. Mixing water

The local tap water in compliance with TCVN 4506: 2012 (2012) was used for the mixing process.

2.1.4. Mixture proportions

All the ANLC mixtures (Table 2) were designed following the procedures described previously by the authors (Nguyen et al., 2022). In detail, FA and GGBFS were used as an alkali-activated binder at a fixed FA/GGBFS ratio of 30/70. The alkali equivalent (AE), alkali modulus (Ms), and a liquid-to-solid ratio of 5%, 0.8, and 0.42, respectively, were applied for all ANLC mixtures. The effect of UCG on the properties of ANLC specimens was investigated by partially replacing BA with UCG at different levels of 5%, 10%, 15%, 20%, 25%, and 30% (by volume), respectively.

shrinkage, and water absorption at 7 and 28 days. In detail, the dry density of ANLC was determined using 50×50×50 mm cubic samples based on TCVN 3121-10:2022 (2022). Also, the flexural strength was measured using specimens with dimensions of 40×40×160 mm, and the halves of the broken samples from the flexural strength test were then used for testing compressive strength following TCVN 3121-11:2022 (2022). Besides, the water absorption rate of ANLC was measured on the 50×50×50 mm specimens following TCVN 3121-18:2003 (2003), while drying shrinkage was recorded at 3, 7, 14, and 28 days using the 25×25×250 mm specimens according to TCVN 8824:2011 (2011). The relationships among the ANLC’s properties were further established to provide an objective view of the impact of the UCG on the performance of the ANLC. Finally, the potential applications of ANLC in real practice were also suggested based on the experimental results.

3. RESULTS AND DISCUSSION

3.1. Dry density

Figure 3 illustrates the dry density of ANLC. The

data reveals that the lowest dry density of 1184 kg/m<sup>3</sup> was recorded for the C30 sample, which contained the highest amount of UCG (30%). Conversely, the sample with 5% UCG exhibited the highest dry density of 1671 kg/m<sup>3</sup>. As a result, dry density decreases as the UCG content increases. Notably, the control sample (C00) had a dry density of 1665 kg/m<sup>3</sup>. The C05 sample had a slightly higher dry density of 6 kg/m<sup>3</sup>, while the dry densities of samples C10, C15, C20, C25, and C30 were progressively lower by 117, 231, 348, 448, and 481 kg/m<sup>3</sup>, respectively. This trend aligns with a previous study (Mohamed & Djamila, 2018). The much lower density of UCG in comparison with BA (as previously mentioned in Section 2.1.2) explains the reduction in dry density of ANLC as increasing UCG content in the mixtures. Moreover, the dry density of ANLC showed an increased trend during the curing ages, which was attributable to the pozzolanic reaction of GGBFS and FA in the system, forming secondary C-S-H gel, enhancing the microstructure, and consequently increasing the dry density of the ANLC specimens.

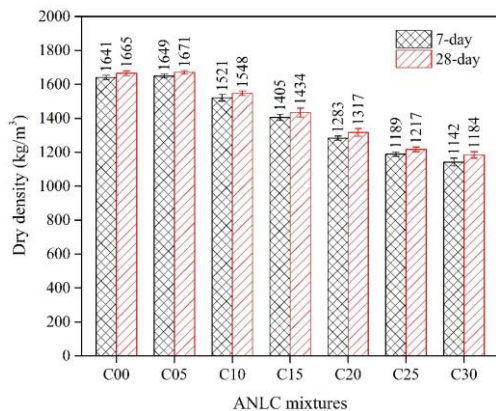


Figure 3. Dry density of ANLC

### 3.2. Flexural strength

Flexural strength is a critical parameter for assessing the performance of ANLC, especially under bending stresses. Generally, the flexural strength of ANLC containing UCG was lower than that of the C00 at all curing ages, except for the C05 specimen (Figure 4). In detail, the C00 registered a flexural strength value of 5.34 MPa at 7 days, and 6.23 MPa at 28 days, while the flexural strength value of the C05 was nearly 14% higher than that of the C00. Replacing 10-30% BA by UCG caused the loss in flexural strength of the ANLC specimens as compared to the UCG-free specimen. For example, the 28-day flexural strength values of the samples with 10, 15, 20, 25, and 30% UCG were 5.37, 3.25, 1.62, 0.57, and 0.41 MPa, which showed a reduction of approximately

14, 48, 74, 90, and 93%, respectively. Previous studies have reported that UCS had a more porous structure and higher water absorption capacity than BA particles (Guendouz et al., 2023; Kua et al., 2016; Wongsa et al., 2017). Consequently, replacing BA with UCG would increase the total void volume in the system and thus decrease the flexural strength of the ANLC. Furthermore, the chemical composition of BA was similar to that of FA, containing high percentages of SiO<sub>2</sub> and Al<sub>2</sub>O<sub>3</sub> (Mohammed et al., 2021; Siddique, 2013), which could also participate in a low-activity pozzolanic reaction of the matrix (Jaturapitakkul & Cheerarat, 2003). In contrast, the primary constituents of UCG were carbone, hydrogen, and azotes (Mohamed & Djamila, 2018), which did not contribute to strength development. Thus, the replacement of BA with UCG limits the chemical reaction, leading to lower ANLC's flexural strength.

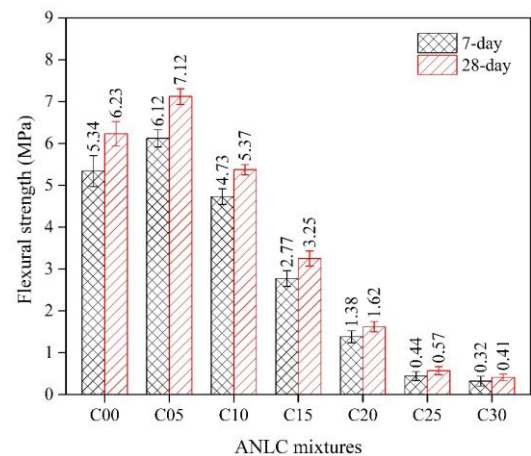


Figure 4. Flexural strength of ANLC

### 3.3. Compressive strength

The compressive strength development of ANLC is illustrated in Figure 5, showing a similar trend to the flexural strength change, as mentioned in Section 3.2. The C05 specimens always earned the highest compressive strength and the strength values of the ANLC specimens containing 10, 15, 20, 25, and 30% UCG were about 17, 58, 74, 93, and 96% lower than that of the no UCG specimen at 28 days. As aforementioned, the involvement of FA, GGBFS, and BA in chemical reactions enhanced the compressive strength of the ANLC after 28 days. Besides, the strength reduction due to the inclusion of UCG could be attributed to the difference in porosity and chemical proportions between BA and UCG as in the above discussion.

The relationship between compressive and flexural strengths was analyzed as shown in Figure 6, proving

that compressive strength was strongly associated with the flexural strength of the ANLC with  $R^2 > 98\%$ . The linear formula of  $y = 5.61x - 1.31$  could be used to estimate either compressive strength or flexural strength at 28 days when one of the two factors was known.

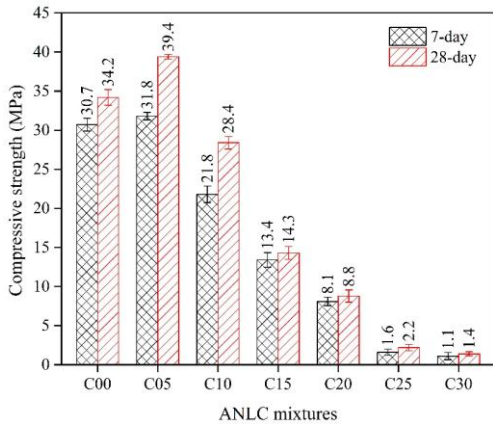


Figure 5. Compressive strength of ANLC

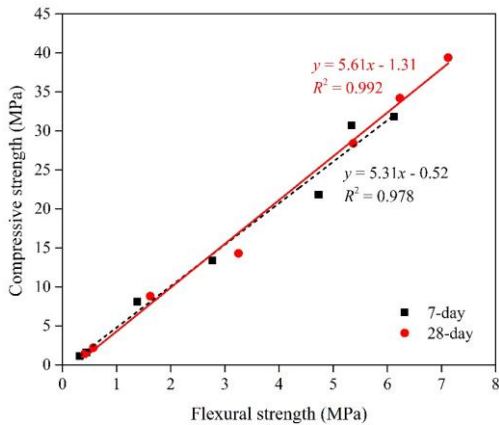


Figure 6. Correlation between compressive and flexural strengths of ANLC

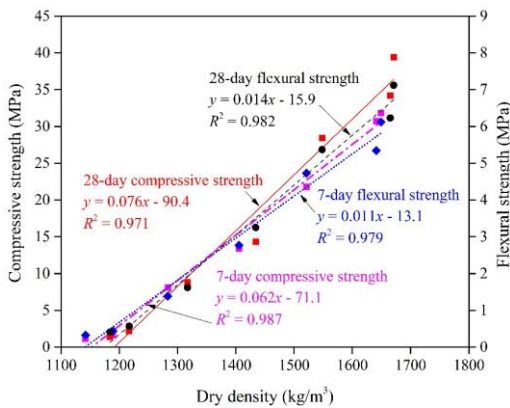


Figure 7. Correlation between dry density and strength of ANLC

The relationship between compressive strength and dry density of the ANLC was also established, as shown in Figure 7. It can be reported that specimens with higher density exhibited greater strength. This finding aligns with the trend discussed in Sections 3.1-3.3. The incorporation of the UCG significantly influenced the microstructure and density of the ANLC, which adversely affected their engineering performance. Besides, the positive correlation between density and strength focused on the importance of optimizing the mixture design to achieve the desired characteristics of ANLC for specific applications.

### 3.4. Drying shrinkage

Drying shrinkage is another crucial characteristic of ANLC, which determines the cracking generation and influences the durability of the component. The drying shrinkage of ANLC samples is illustrated in Figure 8. Notably, the length change of all UCG-incorporated specimens was significantly smaller than that of the control sample at all ages, indicating the positive contribution of UCG in reducing drying shrinkage. This finding could be explained by the following reasons: (1) the surface of UCG particles was jagged with irregular shapes (Kua et al., 2016; Wongsu et al., 2017), improving the mechanical interlocking within the matrix, restricting the movement of the matrix during the drying process, and thus reducing drying shrinkage; (2) UCG particles had a highly porous structure (Guendouz et al., 2023), which absorbed and retained water within the system. This retained moisture helps to reduce the rate and extent of drying shrinkage by providing additional internal curing (Chung et al., 2021); (3) the sizes of UCG particles were smaller than BA particles, thus UCG may act as a filler in the system, effectively reducing the overall paste volume that undergoes shrinkage.

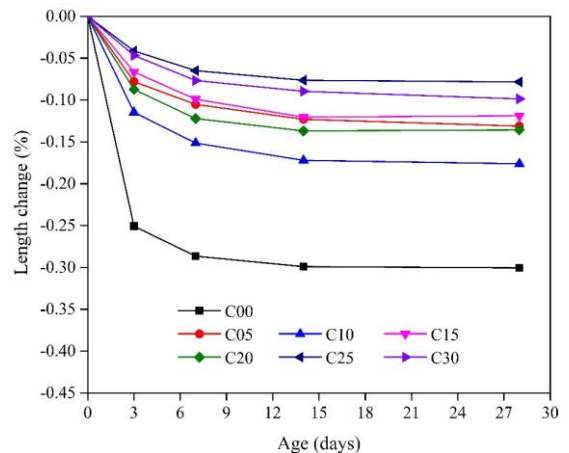
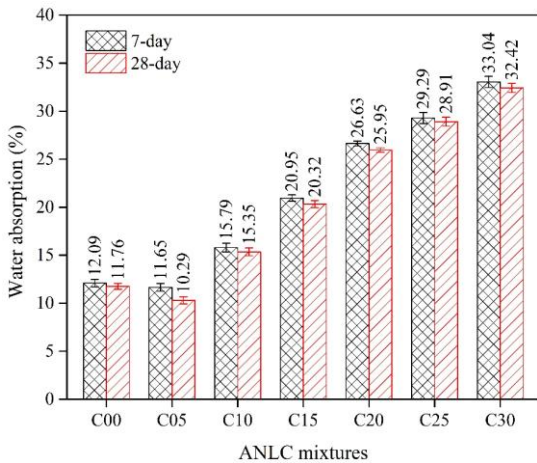


Figure 8. Drying shrinkage of ANLC

**3.5. Water absorption**

The water absorption of ANLC is shown in Figure 9. Overall, most UCG specimens exhibited higher water absorption than the C00 sample, except for the C05 with the smallest water absorption rate of 11.65 and 10.29% at 7 and 28 days, respectively. Further replacing BA with UCG at above 5% resulted in increasing water absorption of the ANLC and the higher the UCG content, the greater the water absorption rate. For instance, the C00 specimens showed a water absorption of 11.76% at 28 days, whereas the C05, C10, C15, C20, C25, and C30 specimens registered respective water absorption levels of 15.35, 20.32, 25.95, 28.91, and 32.42%. Water absorption was directly related to porosity, which inversely affects mechanical strength. The increased porosity due to higher UCG content with porous structure led to higher water absorption and consequently reduced mechanical strength (Nguyen et al., 2022.). In the case of the C05 specimen, it is assumed that 5% UCG was optimal for the filling effect, resulting in a denser structure and preventing the penetration of water (Lee et al., 2023). At higher UCG contents, however, the filling effect was overshadowed by the predominant amount of voids, leading to higher water absorption capacity of the ANLC. Mohamed and Djamilia (2018) reported that the porosity increased after adding more UCG content due to the poor adhesion between the UCG surface and binder. Chung et al. (2021) also proved that the highly porous structure of UCG particles led to higher water absorption of the resulting materials.



**Figure 9. Water absorption of ANLC**

This investigation found that the variation in water absorption with increasing UCG content was in good agreement with the results observed in Sections 3.1-3.3. A close observation of the relationship between

water absorption and the mechanical strength of the ANLC (Figure 10) shows that water absorption was inversely proportional to compressive and flexural strengths. As mentioned above, the increased porosity of the system due to the presence of more UCG led to higher water absorption, associated with lower compressive and flexural strengths. This is indicated by a relatively high correlation coefficient ( $R^2 > 96\%$ ) between water absorption and strength.

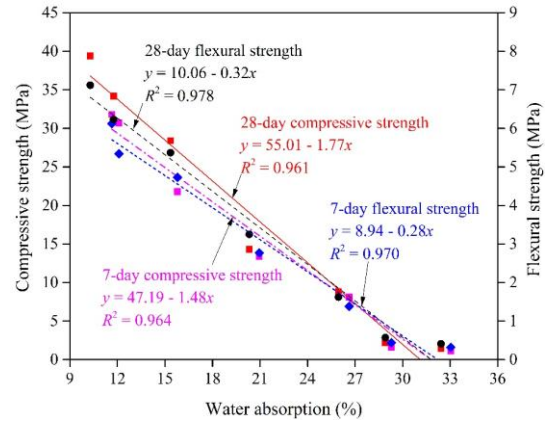


**Figure 10. Correlation between water absorption and strength of ANLC**

**3.6. Application potential of ANLC**

Based on the experimental results presented in the previous sections, ANLC exhibited relatively lower mechanical strength, which is suitable for application in the production of non-load-bearing elements (i.e., bricks and blocks, panels, slabs, etc.). In previous investigations, the UCG was used as raw material for making bricks, thermal insulators (i.e., panels and light steel frame walls), and non-load-bearing partition walls (Khetata et al., 2020; Moutassem & Alamara, 2021). Besides, ANLC may also be used in sound-absorbing applications, such as precast panels and cold-pressed panels, due to the increase in the sound-absorbing potentiality (Saberian et al., 2021).

**4. CONCLUSION**

Based on the experimental outcomes and the associated discussions, the following conclusions may be considered:

- (i) The dry density of ANLC specimens ranged from 1184 kg/m<sup>3</sup> to 1671 kg/m<sup>3</sup> at 28 days. The dry density values tended to be lower when higher UCG content was added to the ANLC mixtures.
- (ii) Replacing 5% of BA with UCG resulted in the maximum flexural and compressive strengths of 7.12 MPa and 39.4 MPa (at 28 days), respectively.

Further BA substitution caused a reduction in the ANLC's strength.

(iii) The inclusion of UCG positively reduced the drying shrinkage of the ANLC. It is a fact that all the ANLC specimens, regardless of the UCG content, exhibited a significantly lower drying shrinkage than the control specimen.

(iv) The 28-day water absorption values of the ANLC specimens were in the range of 10.29-32.42%, which is about 3.5-20% higher than that of the control specimen. Increased UCG content correlates with increased water absorption in ANLC, except for the 5% UCG specimen, which exhibited the lowest absorption rate at 10.29%.

(v) The ANLC prepared in this study can be applied

for the production of non-load-bearing elements, such as bricks and blocks, wall and slab panels, non-load-bearing partition walls, and sound-absorbing panels. The results of this investigation demonstrated the high and wide application potential of ANLC in real practice.

### CONFLICT OF INTEREST

The authors declare that they have no known competing financial interests or personal relationships that may appear to influence the work reported in this paper.

### ACKNOWLEDGMENT

This study is funded by the Can Tho University, Code: THS2024-55.

### REFERENCES

- Busch, P. F., & França Holanda, J. N. (2022). Potential use of coffee grounds waste to produce dense/porous bi-layered red floor tiles. *Open Ceramics*, 9, 100204. <https://doi.org/10.1016/j.oceram.2021.100204>
- Chung, L. L. P., Wong, Y. C., & Arulrajah, A. (2021). The application of spent coffee grounds and tea wastes as additives in alkali-activated bricks. *Waste and Biomass Valorization*, 12(11), 62736291. <https://doi.org/10.1007/s12649-021-01453-7>
- Darvish, P., Johnson Alengaram, U., Soon Poh, Y., Ibrahim, S., & Yusoff, S. (2020). Performance evaluation of palm oil clinker sand as replacement for conventional sand in geopolymer mortar. *Construction and Building Materials*, 258, 120352. <https://doi.org/10.1016/j.conbuildmat.2020.120352>
- Nguyen, T. H. Y., Cao, N. T., Tran, D. M. N., & Huynh, T. P. (2022). Experimental evaluation on engineering properties and drying shrinkage of no-cement mortar produced by alkaline activation of fly ash-slag mixtures. *Engineering Journal*, 26(3), 17–28. <https://doi.org/10.4186/ej.2022.26.3.17>
- Gencil, O., Gholampour, A., Tokay, H., & Ozbakkaloglu, T. (2021). Replacement of natural sand with expanded vermiculite in fly ash-based geopolymer mortars. *Applied Sciences*, 11(4), 4. <https://doi.org/10.3390/app11041917>
- Ghosh, P., & Venkatachalapathy, N. (2014). Processing and drying of coffee – A review. *International Journal of Engineering Research and Technology*, 3(12), 784–794. <https://www.ijert.org/research/processing-and-drying-of-coffee-a-review-IJERTV3IS120482.pdf>
- Guendouz, M., Boukhelkhal, D., Triki, Z., Mechantel, A., & Boukerma, T. (2023). Effect of using spent coffee grounds wastes as aggregates on physical and thermal properties of sand concrete. *Algerian Journal of Environmental Science and Technology*, 9(3), 3256–3264. <https://www.aljest.net/index.php/aljest/article/view/894>
- Jaturapitakkul, C., & Cheerarat, R. (2003). Development of bottom ash as pozzolanic material. *Journal of Materials in Civil Engineering*, 15(1), 48–53. [https://doi.org/10.1061/\(ASCE\)0899-1561\(2003\)15:1\(48\)](https://doi.org/10.1061/(ASCE)0899-1561(2003)15:1(48))
- John, S. K., Nadir, Y., & Girija, K. (2021). Effect of source materials, additives on the mechanical properties and durability of fly ash and fly ash-slag geopolymer mortar: A review. *Construction and Building Materials*, 280, 122443. <https://doi.org/10.1016/j.conbuildmat.2021.122443>
- Khetata, S. M., Piloto, P. A., & Gavilán, A. B. (2020). Fire resistance of composite non-load bearing light steel framing walls. *Journal of Fire Sciences*, 38(2), 136–155. <https://doi.org/10.1177/0734904119900931>
- Kua, T.-A., Arulrajah, A., Horpibulsuk, S., Du, Y.-J., & Shen, S.-L. (2016). Strength assessment of spent coffee grounds-geopolymer cement utilizing slag and fly ash precursors. *Construction and Building Materials*, 115, 565–575. <https://doi.org/10.1016/j.conbuildmat.2016.04.021>
- Lee, J. dong, Kim, J., & Lee, S. (2023). Study of recycled spent coffee grounds as aggregates in cementitious materials. *Recent Progress in Materials*, 5(1), 1. <https://doi.org/10.21926/rpm.2301007>
- Mohamed, G., & Djamila, B. (2018). Properties of dune sand concrete containing coffee waste. *MATEC Web of Conferences*, 149, 01039. <https://doi.org/10.1051/matecconf/201814901039>
- Mohammed, S. A., Koting, S., Katman, H. Y. B., Babalghaith, A. M., Abdul Patah, M. F., Ibrahim, M. R., & Karim, M. R. (2021). A review of the utilization of coal bottom ash (CBA) in the

- construction industry. *Sustainability*, 13(14), 14. <https://doi.org/10.3390/su13148031>
- Moussa, T., Maalouf, C., Bliard, C., Abbes, B., Badouard, C., Lachi, M., do Socorro Veloso Sodré, S., Bufalino, L., Bogard, F., Beaumont, F., & Polidori, G. (2022). Spent coffee grounds as building material for non-load-bearing structures. *Materials*, 15(5), 5. <https://doi.org/10.3390/ma15051689>
- Moutassem, F., & Alamara, K. (2021). Design and production of sustainable lightweight concrete precast sandwich panels for non-load bearing partition walls. *Cogent Engineering* 8, 1993565. <https://doi.org/10.1080/23311916.2021.1993565>
- Nab, C., & Maslin, M. (2020). Life cycle assessment synthesis of the carbon footprint of Arabica coffee: Case study of Brazil and Vietnam conventional and sustainable coffee production and export to the United Kingdom. *Geo: Geography and Environment*, 7(2), e00096. <https://doi.org/10.1002/geo2.96>
- Roychand, R., Kilmartin-Lynch, S., Saberian, M., Li, J., Zhang, G., & Li, C. Q. (2023). Transforming spent coffee grounds into a valuable resource for the enhancement of concrete strength. *Journal of Cleaner Production*, 419, 138205. <https://doi.org/10.1016/j.jclepro.2023.138205>
- Saberian, M., Li, J., Donnoli, A., Bonderenko, E., Oliva, P., Gill, B., Lockrey, S., & Siddique, R. (2021). Recycling of spent coffee grounds in construction materials: A review. *Journal of Cleaner Production*, 289, 125837. <https://doi.org/10.1016/j.jclepro.2021.125837>
- Scalia, L. G., Saeli, M., Miglietta, P. P., & Micale, R. (2021). Coffee biowaste valorization within circular economy: An evaluation method of spent coffee grounds potentials for mortar production. *The International Journal of Life Cycle Assessment*, 26(9), 1805–1815. <https://doi.org/10.1007/s11367-021-01968-0>
- Schmidt Rivera, X. C., Gallego-Schmid, A., Najdanovic-Visak, V., & Azapagic, A. (2020). Life cycle environmental sustainability of valorisation routes for spent coffee grounds: From waste to resources. *Resources, Conservation and Recycling*, 157, 104751. <https://doi.org/10.1016/j.resconrec.2020.104751>
- Siddique, R. (2013). Compressive strength, water absorption, sorptivity, abrasion resistance and permeability of self-compacting concrete containing coal bottom ash. *Construction and Building Materials*, 47, 1444–1450. <https://doi.org/10.1016/j.conbuildmat.2013.06.081>
- Srividya, T., Kannan R. P. R., Sivasakthi, M., Sujitha, A., & Jeyalakshmi, R. (2022). A state-of-the-art on development of geopolymer concrete and its field applications. *Case Studies in Construction Materials*, 16, e00812. <https://doi.org/10.1016/j.cscm.2021.e00812>
- Suksiripattanapong, C., Krosoongnern, K., Thumrongvut, J., Sukontasukkul, P., Horpibulsuk, S., & Chindaprasirt, P. (2020). Properties of cellular lightweight high calcium bottom ash-portland cement geopolymer mortar. *Case Studies in Construction Materials*, 12, e00337. <https://doi.org/10.1016/j.cscm.2020.e00337>
- Ministry of Science and Technology (Vietnam). (2022). *Mortar for masonry - Test methods - Part 10: Determination of dry bulk density of hardened mortars* (TCVN 3121-10:2022). <https://storethinghiem.vn/tcvn-3121-10-2022>
- Ministry of Science and Technology (Vietnam). (2022). *Mortar for masonry - Test methods - Part 11: Determination of flexural and compressive strength of hardened* (TCVN 3121-11:2022). <https://storethinghiem.vn/uploads/files/TCVN3121-11-2022.pdf>
- Ministry of Science and Technology (Vietnam). (2003). *Mortar for masonry - Test methods - Part 18: Determination of water absorption of hardened mortars* (TCVN 3121-18:2003). <https://storethinghiem.vn/uploads/files/tcvn-3121-2003.pdf>
- Ministry of Science and Technology (Vietnam). (2012). *Water for concrete and mortar - Technical specifications* (TCVN 4506:2012). [https://maykiemdinh.vn/tai-lieu/tcvn-45062012-yeu-cau-ky-thuat-nuoc-cho-be-tong-va-vua-114.html#google\\_vignette](https://maykiemdinh.vn/tai-lieu/tcvn-45062012-yeu-cau-ky-thuat-nuoc-cho-be-tong-va-vua-114.html#google_vignette)
- Ministry of Science and Technology (Vietnam). (2011). *Cements - Test method for drying shrinkage of mortar* (TCVN 8824:2011). <https://luatminhkhue.vn/tieu-chuan-quoc-gia-tcvn-8824-2011-ve-xi-mang-phuong-phap-xac-dinh-do-co-kho-cua-vua.aspx>
- Torga, G. N., & Spers, E. E. (2020). Chapter 2— Perspectives of global coffee demand. In L. F. de Almeida & E. E. Spers (Eds.), *Coffee consumption and industry strategies in Brazil* (pp. 21–49). Woodhead Publishing. <https://doi.org/10.1016/B978-0-12-814721-4.00002-0>
- Wongsa, A., Boonserm, K., Waisurasingha, C., Sata, V., & Chindaprasirt, P. (2017). Use of municipal solid waste incinerator (MSWI) bottom ash in high calcium fly ash geopolymer matrix. *Journal of Cleaner Production*, 148, 49–59. <https://doi.org/10.1016/j.jclepro.2017.01.147>
- Zeyad, A., Megat Johari, M. A., Bakar, B. H., Mijarsh, M., & Ahmad, Z. (2020). Influence of SiO<sub>2</sub>, Al<sub>2</sub>O<sub>3</sub>, CaO, and Na<sub>2</sub>O on the elevated temperature performance of alkali-activated treated d palm oil fuel ash-based mortar. *Structural Concrete*, 22(1), 1–20. <https://doi.org/10.1002/suco.201900302>